Exploration and Visualisation of full-waveform LiDAR data for forestry applications

Milto Miltiadou*[1,2,3], Neil DF Campbell[1], Matthew Brown[1], Susana Gonzalez Aracil[3], Mark Warren[2], Darren Cosker[1], Daniel Clewley[2]andMichael Grant[2]

[1]The Centre for Digital Entertainment, University of Bath, UK
[2]Remote Sensing Group,Plymouth Marine Laboratory, UK
[3]Interpine Group Ltd, Rotorua, NZ

15/11/2016

*Corresponding author

Abstract

This study focuses on enhancing the visualisations and classifications of forested areas using coincident full-waveform (fw) LiDAR data and hyperspectral images. The ultimate aim is use both datasets to derive information about forests and show the results on a 3D virtual, interactive environment. Influenced by Persson et al (2005), voxelisation is an integral part of this research. The intensity profile of each full-waveform pulse is accumulated into a voxel array, building up a 3D density volume. The correlation between multiple pulses into a voxel representation produces a more accurate representation, which confers greater noise resistance and it further opens up possibilities of vertical interpretation of the data. The 3D density volume is then aligned with the hyperspectral images using a 2D grid similar to Warren et al (2014) and both datasets are used in visualisations and classifications.

Previous work in visualising fw LiDAR has used transparent objects and point clouds, while the output of this system is a coloured 3D-polygon representation, showing well-separated structures such as individual trees and greenhouses. The 3D density volume, generated from the fw LiDAR data, is polygonised using functional representation of object (FReps) and the marching cubes algorithm (Pasko and Savchenko, 1994) (Lorensen and Cline, 1987). Further, an optimisation algorithm is introduced that uses integral volumes (Crow, 1984) to speed up the process of polygonising the volume. This optimisation approach not only works on non-manifold object, but also a speed up of up to 51% was achieved. The polygon representation is also textured by projecting the hyperspectral images into the mesh. In addition, the output is suitable for direct rendering with commodity 3D-accelerated hardware, allowing smooth visualisation.

In future work, the effects of combining both hyperspectral imagery and fw LiDAR in classifications and visualisations are examined. At first, two pixel wise classifiers, a support vector machine and a Bayesian probabilistic model, will be used for testing the effects of the combination in generating tree coverage maps. Higher accuracy classification results are expected when metrics from both datasets are used together. Regarding the visualisations, the differences of applying surface reconstruction versus direct volumetric rendering will be discussed and an ordered tree structure with integral sums of the node values will be used for speeding up the ray-tracing of direct volumetric rendering and improving memory management of aforementioned optimisation algorithm with integral volumes. Further, deferred rendering is suggested for testing the visual human perception of projecting multiple bands of the hyperspectral images on the FW LiDAR polygon representations. At the end of this project the combination of the datasets will be used along with the watershed algorithm for tree segmentation, which is useful for measuring the stem density of a forest and for tree species classifications.

Acknowledgements

Above all, I would like to express my great gratitude to my industrial supervisors Dr. Michael Grant who had supported me continuously during my research and gave me the freedom to create a project of my own interest.

Then, I would like to thanks Dr. Matthew Brown, who helped me during my first years of my studies by giving me valuable and informative feedback. He was always there to keep me working on the right track.

Equally important is my current supervisor Dr. Neil DF Campbell and he is not to be missed from the acknowledgements.

Furthermore, special thanks are given to Dr. Mark Warren, Dr. Daniel Crewely, Dr. Darren Cosker, MSc Susana Gonzalez Aracil and Dr. Ross Hill who occasionally advised me during my studies.

It further worth giving credits to my data providers, the Natural Environment Research Council's Airborne Research and Survey Facility (NERC ARSF) and Interpine Group Ltd.

Last but not least, I am extremely grateful to my funding organisations, the Centre for Digital Entertainement and Plymouth Marine Laboratory, who supported financially and consequently made this research possible.

Contents

1 Introduction

This research aims to ease the way of handling full-waveform (FW) LiDAR data for remote forest surveys. Automated ways of monitoring forests are required to reduce the time consuming and expensive fieldwork undertaken for monitoring both commercial and sustainable forests. The discrete LiDAR has been widely used and a 40% reduction of fieldwork has been achieved at Interpine Ltd Group, New Zealand, with that technology. FW LiDAR systems are novel in that they record the entire backscatter signal of the emitted pulse, rather than a few returns common with conventional discrete LiDAR. This suggests many new problems and possibilities from the point of view of image understanding, remote surveying and visualisation. Scientists understand their concepts and potentials but due to the lack of available tools able to handle these large datasets, there are very few uses of FW LiDAR [3].

The primary output of this thesis is the open source software DASOS (=forest in Greek), which aims to break the barrier between understanding and using the FW LiDAR. New representations of the FW LiDAR are further proposed for handling the data and by using those representations, DASOS can produce 3D polygons and metrics useful in deriving information about the scanned areas. The contributions of the DASOS and the new representations of the FW LiDAR are demonstrated in three applications: alignment with hyperspectral imagery, dead tree detection and optimised volumetric visualisation.

1.1 Motivation

Importance of Forest Monitoring and Applications

- Forest Health: Detecting tree diseases at early stages and treat trees Potential protection of vegetation from diseases and pests [1]. An example of pests, which destroy vegetation, is the Brushtail Possums, which were initially brought to New Zealand for fur trade, but they have escaped and they are a thread to native forests and vegetation [2]. Measuring the effect on the forest health is difficult. The Landcare Research and Department of Conservation (DOC), in cooperation with Aberystwyth University, collected full-waveform LiDAR data from the North Island of New Zealand to investigate those effects. But according to Dr Pete Bunting, who is involved in that research, there are no available tools to those organisations for reading and processing full-waveform LiDAR data (personal communication).

- Biodiversity Management - Tree hollows - Estimating the value of a commercial forest - wood trade - Archaeology: structure below dense forest lead into the detection of ancient hidden city in Cambodian jungle [10] - Woodland Phenology: by observing the change in number of trees species, the recurring of natural phenomena can be predicted and potentially pre‘vented [5].

Fieldwork - time consuming

LiDAR refers to the acquisition of information from laser scanners. There are two types of LiDAR data, the discrete and the full-waveform (FW). The discrete LiDAR measures the round trip distance time of the laser beam and calculates the position of a few hit points, while the FW LiDAR records the entire backscattered signal. But the increased amount of information recorded within the FW LiDAR makes handling of those data difficult. As an indication, a 9.3GB discrete LiDAR from New Forest, UK, corresponds to 55.7GB of FW LiDAR. The discrete LiDAR has been widely used and a 40% reduction of fieldwork has been achieved at Interpine Ltd Group, New Zealand, with that technology. Regarding the FW LiDAR, scientists understand their concepts and potentials but due to the lack of available tools able to handle these large datasets, there are very few uses of FW LiDAR [3]. , which aims to break the barrier between understanding and using the FW LiDAR.

and by using those representations DASOS can produce 3D polygons and metrics useful

in deriving information about the scanned areas.

:

Firstly, a new and fast way of aligning the FW LiDAR with Remotely Sensed Images has been developed in DASOS and by generating tree coverage maps it was shown that the combination of those datasets confers better remote survey results. This work was presented at the 36th ISRSE International Conference.

Secondly, automated detection of dead trees in native Australian forests has a significant role in protecting animals, which live in those trees and are close to extinction. DASOS allow the generation of 3D signatures characterising dead trees. A comparison between the discrete and FW LiDAR is performed to demonstrate the increased survey accuracy obtained when the FW LiDAR are used.

Finally, the last application is for improving visualisations for foresters. Foresters have a great knowledge about forests and can derive a wealth of information directly from visualisations of the remotely sensed data. This reduces the travelling time and cost of getting into the forests. This research optimises visualisations by using the new FW LiDAR representations and a speed of up to 51% has been achieved.

FW LiDAR has great potentials in forestry and this research has already started to have an impact in the FW LiDAR community by making those huge datasets easier to handle. DASOS is now used at Interpine Group Ltd, a world leading Forestry Company in New Zealand and it has been tested from a PhD student at Bournemouth University who looks into estimating bird distribution in the New Forest. In the future, it is expected that DASOS will be widely used in remote forest surveys (i.e. estimating the commercial value of a forest and detecting infected trees at early stages for treatment).

1.2 Aims and Objectives

The overarching aim of future work is to improve and optimise visualisations of full-waveform LiDAR data and hyperspectral images for remote forest surveying.

Objectives:
1. Enable browsing of very large scale datasets with many points and spectral bands in an efficient manner 2. Estimate tree coverage and investigate the potential of integrating multiple remote sensing datasets in forestry 3. Tree crown detection and height estimations in comparison to human detection, which will benefits wood trade and forest management 4. Enable experts to establish wood coverage 5. Enable understanding of forestry concepts through 3D visualisations 6. Investigate data structures that will be better for volumetric rendering and efficient management of large point clouds

This project explores visualisation and data-understanding for full waveform LIDAR systems.

- How can large full waveform datasets be effectively and efficiently visualised? (especially in combination with other forms of data, such as hyperspectral images). - How can terrain classification systems can be modified to effectively make use of full-waveform data? (for example, detection of dead trees for protecting animals living inside dead trees in Australia). - Can visualisation and classification be improved by inference of high quality 3D information, for example, using priors over the space of 3D elements and compatibility between multiple observations? The project will also encompass other facets of large volume environmental dataset visualisation and understanding as appropriate.

1.3 Background

Full-waveform LiDAR data are airborne remote sensing data. Remote sensing refers to acquisition of information about objects, like vegetation and archaeological monuments,

without physical contact and the interpretation of that information. The sensors used to capture the information are divided into passive and active. For example satellites are passive sensors because they collect information from the sun light, while Airborne Laser Scanners (ALS) are active because they emit a laser pulse and collects information from its returns [17].

According to Wanger et al, Airborne Laser Scanning (ALS) is a growing technology used in environmental research to collect information about the earth like vegetation and tree species. Comparing ALS with traditional photography scanning, ALS is more flexible because it is not influenced by light and it can collect information from below the tree canopies [19]. ALS are divided into pulse systems and continuous wavelength systems. Continuous wavelength systems are more complicated, because they obtain one extra physical parameter. Further, according to Wehr and Lohr continuous wavelength Systems are 85 times less accurate than pulse systems [20].

Laser radars are ALS systems that are able to obtain range images by repeatedly emitting pulses. Those systems are commonly known as LiDAR (Light Detection and Ranging) [20]. Full-waveform LiDAR can encode and store the entire radiation returned from each pulse, digitised over time. The design of the first FW LiDAR system was introduced in 1980s, but the first operational system was developed by NASA in 1999 [6]. There are two types of LiDAR systems: small-footprint and large-footprint. On the one hand, small-footprint returns a higher detailed accuracy but it cannot guarantee that the pulse will reach the ground, making height related calculations difficult. On the other hand, since the diameter of large-footprint scanners is much bigger, they are able to scan wider areas and the last target is much more likely to be the ground [12].

The most common approach of interpreting the FW LiDAR from the Leica instrucment is to decompose the waveform into a sum of Gaussian functions, each representing a peak return, and sequentially extract point clouds from [18]. Neunschwander et al (2009) used this approach for Landcover classification while Reitberger et al (2006) applied it for distinguishing deciduous trees from coniferous trees [14] [16]. In 2007, Chauve et al proposed an approach of improving the Gaussian model in order to increase the density of the points extracted from the data and consequently improve point based classifications applied on FW LiDAR data [6].

Nevertheless, the state-of-art sensors, RIEGL LMS-Q780 and RIEGL LMS-Q680i are native full-waveform sensors. Therefore, the discrete LiDAR are produced by extracting peak points at post-processing. The Gaussian decomposition used to extract points from full-waveform at the aforementioned papers [?] is now used before the data are delivered. Therefore the concept of extracting a denser point clouds using Gaussian decomposition does not apply on data from Riegl. That was proved by extracting peak points from RIEGL FW LiDAR data using the pulseextract from LAStools [9]. The number of points extracted was the same as the number of points existed inside the discrete LiDAR files delivered.

new ways of interpreting full-waveform - Cao voxelisation seems the future

[4]

To sum up

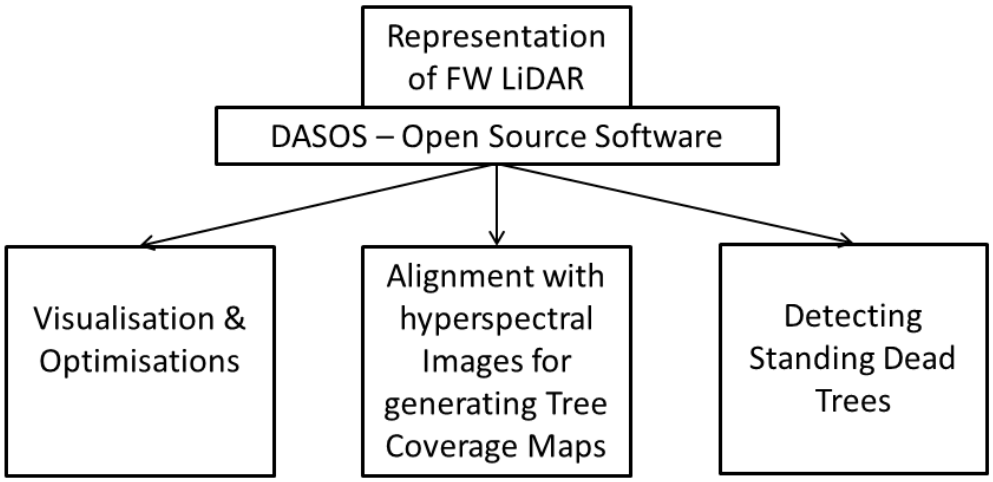

Figure 1: The pipeline of the thesis

2 Pipeline

3 Acquire Data

two organisation: 1. Natural Environment Research Council's Airborne Research and Survey Facility (NERC ARSF) 2. Interpine Ltd Group ()

1. used for the hyperspectral Alignment 2. dead tree detection both for visualisations and optimisations of various data structures

3.1 Instrumenets

1. Instruments - Leica ALS50-II - AISA Eagle and Hawk

2. Instrument - Riegl LMS-Q680i

The sample data used for this thesis are provided by Natural Environment Research Council's Airborne Research and Survey Facility (NERC ARSF). The datasets mainly used were scanned on the 8th of April in 2010 at New Forest in UK. For every flightline, two Airborne Remote Sensing datasets are given:

- Full-waveform (FW) LiDAR data collected from the Leica ALS50-II system - Hyperspectral Images collected from the AISA Eagle and Hawk instruments

For each flightline, there is a FW LiDAR file, as well as the corresponding hyperspectral data. But since the data are collected from different instruments they are not aligned (see section 5 for more information on aligning the data).

In the following sub-sections, background information on the input datasets is given, starting from simple concepts like Remote Sensing. Then, the inputs are explained in practise; what the actual input data are and how they are interpreted. The challenges of dealing with the data are also outlined and discussed.

3.2 Full-waveformLiDAR

3.3 Hyperspectral Imagery

4 Representations of Data

TODO::START:
Aim - > move forward and manipulate FW LiDAR into a more native format instead of extracting points. As mentioned before Riegl is a native FW system and since the same algorithm are used no difference in the numbers of discrete points and points extracted from pulseextra.exe from LAStools was found.

In this thesis, I showed that FW LiDAR data can be used for both visualising and extracting information after voxelisation. TODO::END:

4.1 3D Volume

TODO::START:
rewrite the following: - Voxels - how are they generate - Normalisation: each sample intensity represents the amount of radiation return into a constant time interval. Therefore to normalise the intensities across the voxels the average of the number of samples added to the voxels is taken. Example if 5 samples are inside a voxels and the waveform is digitised at 2ns, therefore 10ns internal of waveform is saved into that voxels. To keep it consistent the length of waveform across the voxels the average intensity of the number of samples inserted into each voxel is taken.

Similar to Person et al, the waveforms are converted into voxels by inserting the waves into a 3D discrete density volume. But in this approach the noise is removed by a threshold first. When a pulse doesn't hit any objects, the system captures low signals which are noise. For that reason, the samples with amplitude lower than the noise level are discarded. Further, to overcome the uneven number of samples per voxel, the average amplitude of the samples that lie inside each voxel is taken, instead of selecting the sample with the highest amplitude [15]:

$$I_v = \frac{\sum_{i=1}^{n} I_i}{n} \tag{1}$$

Where n = number of samples of a voxel, Ii = the intensity of the sample i, Iv is the accumulated intensity of the voxel. The main issue of that approach is that the intensities of the LiDAR data haven't been calibrated. Non calibrated intensities do not significantly affect the creation of polygon meshes, because during polygonisation, the system treats the intensities as Booleans; is that voxel empty or not? Nevertheless, the noise level could be set lower if the intensities were calibrated and more details would be preserved on the polygon meshes. For that reason, calibrating the intensities of the return is a task needing to be performed in order to enable the use of intensities in future classifications.

4.2 Implicit Object

Once the 3D discrete density volume is generated, numerical implicitization of objects is used to represent the scanned area. Numerical implicitization was introduced by Blinn in 1982; A function $f(X)$ defines an object, when for every n-dimensional point X that lies on the surface of the object, satisfied the condition$X = \alpha$. Numerical implicitization allows definition of complex object, which can easily been modified, without saving large amounts of triangles.
The 3D volume, generated as explained in the previous section, is used as a discrete density function $f(X), \alpha$ to represent an object (Pasko and Savchenko, 1994):
f(X) = α , when X lies on the surface of the object
f(X) > α , when X lies inside the object and
f(X) < α , when X lies outside the object
where
X = a 3D point (x, y, z) representing the longitude, latitude and height respectively

f(X) =the discrete density function that takes X as input and returns the accumulated intensity value of the voxel that X lies in
α = the isolevel of the object and defines the boundary of the object.
f(X) is equal to α iff X lies on the surface of the object. The isolevel α is a user defined parameter and varies depending on the amount of noise in the data.

Even though numerical implicitization is beneficial in reducing storage memory and for various resolution renderings of the same object, visualising numerical/algebraic objects is not straight forward, since they contain no discrete values. More information about visualisations are given at Section 5

A big part of this thesis is the way of handing data and how algorithmic approaches can speed up accessing of FW LiDAR data while keeping memory allocation low. The next sections explains the data structures implemented and the new ones proposed during this studies. The functionalities are explained here while their performance is discussed at section 5.

The names of the data structures are the given below. Some names are from standard data structures and the new ones proposed have

1. 1D array
2. 1D hashed array
3. Octree
4. Integral Volumes
5. Integral Tree
6. Hashed OCtree
7. Series of Hashed Octrees

4.3 Integral Volumes

In 1984, Crow proposed an image representation where each pixel value is replaced by the sum of all the pixels that belong to the rectangle defined by the lower left corner of the image and the pixel of our interest (Crow, 1984). Even though more storage space is required to save the image, due to the larger numbers, the sum of every rectangle in the image can be calculated in constant time, once the table is constructed. The integral image can also be constructed in linear time O(n), where n is the number of pixels in the image. One iteration through the entire image is enough to replace the pixel values of the image.

image

5 Visualisations

Even though numerical implicitisation is beneficial in reducing storage memory and for various resolution renderings of the same object, visualising numerical/algebraic objects is not straight forward, since they contain no discrete values. This problem can either be address either by ray-tracing or polygonisation. In 1983, Hanraham suggested a ray-tracing approach, where an equation is derived from the ray and surface intersection. The Marching Cubes algorithm was later introduced for polygonising implicit objects. The algorithm first divides the space into cube and then creates consistent triangle using look up table (Lorensen and Cline, 1987).

The Marching cubes algorithm constructs surfaces from implicit objects using a search table. Let's assume that f(X) defines an implicit object. At first the space is divided into cubes, named voxels. Each voxel is defined by eight corner points, which lie either inside or outside the object. By enumerating all the possible cases and linearly interpolating the intersections along the edges, the surface of the implicit object is constructed (Lorensen and Cline; 1987).

According to Lorensen and Cline, the normal of each vertex is calculated by measuring the gradient change. But in our case, due to the high gradient changes inside the volume, calculating the normal in that way leads to a non-smooth visualisation. For that reason, in this research the normal of each vertex is equal to the average normal of its adjacent triangles.

Further the sampling of the Marching cubes is independent from the sampling of the 3D density volume. Therefore consistency between the two is required and more information about that is given at the results section 4.5.5.

5.1 Optimising Marching Cubes

The original Marching Cubes algorithm uses a scan line approach and processes all the cubes sequentially. The scan line approach sometimes implies looping through large amounts of empty cubes. To optimise the process, in this research, it is proposed an algorithm that repeatedly divides the volume and utilities Integral Volumes to discard empty volumes during the polygonisation. Using this optimisation algorithm it was achieved an up to 51This optimisation algorithm is explained in the following sections, which are structured as follow: - Background information, including previous related work. - How integral images are extended into 3D. - The proposed algorithm of using Integral Volumes to speed up the process of polygonising an implicit object using the Marching Cubes algorithm - Implementation details that contribute to the efficiency and speed up of the algorithm - Results

5.2 Background

Much research has been done so far on optimising and improving the polygonisation of implicit surfaces. But most research is based on closed and manifold object. A polygon mesh is closed when it has no holes and it is manifold when it can be unfolded into a 2D continues surface. In order to guarantee consistent topology, an optimised approach with an enhanced look up table was proposed by Lewiner et al in 2003.

Further surface-tracking was discussed in both papers of (Rodrigues de Araujo and Pires Jorge, 2005) (Hartmann, 1998). Starting from a seed point, the surface is expanded according to the local curvature of the implicit object. Self-intersections and collisions are avoided using heuristic edge length. This method is considered to be faster and more efficient, in comparison with the Marching Cubes algorithm. Because, by tracking the surface, huge empty spaces are not searched and it is also possible to create smaller triangles on places with high gradient changes and bigger triangles on surfaces with low

variance. Nevertheless, surface-tracking Algorithms cannot be applied in our case though, because the output of on my program is a non-manifold objects. The 3D Volume generated from FW LiDAR data is not consistent, since small footprint Leica FW systems cannot guarantee that the last return is from the ground. For that reason, it is possible that some trees may be separated from the ground. Surface-tracking algorithms converge once the object is closed. Therefore, there is a possibility that they may converge after polygonising a single tree if the seed point lies on a tree that is separated from the ground.

In 1992, Hansen and Hinker proposed parallelising the polygonisation process of BlobTree trees on Single Instruction, Multiple Data (SIMD) machines. BlobTree trees represent implicit objects as a combination of primitives and operations likes union and blends (Galbraith, MacMurchy, and Wyvill, 2004). While the depth of the tree increases, the time required to get the value that defines whether a point is inside or outside the object increases as well. On SIMD machines greater speed up is achieved at longer instruction due to the less communication cost. Therefore parallelising the process of BlobTree trees with long depth is beneficial, but in our case the value returned for a given point is calculated in constant time. Further, according to the C++ Coding Standards by Sutter and Alexandrescu, when optimisation is required is better to seek an algorithmic approach first because it is simpler to maintain and the possibility of being bug free is higher (Sutter and Alexandrescu, 2004).

OpenVDB library manages volumetric data with octrees. My program uses 1D arrays allowing constant time access of voxel values and by importing OpenVDB library, its speed was significantly decreased; while the number of voxels is increasing the time required to get the value of a voxel is also increasing. Further according to the documentation, the VolumeToMesh class "meshes any scalar grid that has a continuous isosurface", while the surface of the FW LiDAR volumes is not continuous; there are triangles that represent leafs inside the trees and some of the trees may be disconnected from the ground because the last return do not always reach the earth (OpenVDB 2.3.0).

In this report, it is introduced a new method of optimising the marching cubes algorithm. This method utilises Integral Volumes (an extension of Integral Images) to discard chunks of empty cubes during polygonisation. Its effectiveness stands at the ability of integral volumes to find the sum of any sub-volume into constant time and it is important because it works effectively non-manifold or non-closed objects.

6 Alignment with Hyperspectral Imagery

7 Classifications

This talk presents the new features of DASOS, which is an open source software for managing full-waveform LiDAR data and those features are used for detecting dead standing Eucalypt.

The value of dead standing Eucalypt trees from a biodiversity management perspective is large. In Australia, many arboreal mammals and birds that are close to extinct inhabit hollows [7]. Nevertheless, studies predict shortage of hollows in the near future due to tree harvesting and the decades required for a tree to be mature enough to develop a hollow [11] [8]. Dead standing eucalypt trees are more likely to be aged and have hollows, therefore automated detection of them plays a significant role in protecting animals that rely on hollows.

DASOS (= $\delta\acute{\alpha}\sigma o\varsigma$) means forest in Greek and it is an open source software aiming to ease the way of handling FW LiDAR data in forestry [13]. Traditional ways of interpreting FW LiDAR data, suggests extraction of a denser points cloud using Gaussian decomposition [14] [16]. Nevertheless DASOS was influenced by Persson et al, 2005, who used voxelisation to visualise the waveforms [15]. But, DASOS do not only uses voxelisation for visualisations but also for extracting metrics useful in classification. It further normalises the intensities so that equal pulse length exists inside each voxel, making intensities more meaningful. It is further seems that the literature is moving towards voxelisation with the good results obtained at recent publication on tree species classification [4].

The new features of DASOS: New features of DASOS which enables observation at tree level: i.e. distribution of intensities at specific area

The data, provided by RPS Australia East Pty Ltd, were collected in March 2015 from the Riegl (LMS-Q780 or LMS-Q680i?) sensor at an Australian native Forest with eucalyptus. The fieldplots has been provided by (Interprine Group Ltd or Forest Corporation?).

examined with Random Forest

The new features of DASOS are presented and used for generating 3D signatures characterising dead standing trees and a comparison between the discrete and FW LiDAR data is performed to demonstrate the increased survey accuracy obtained with the FW LiDAR.

8 Overall Results

9 Conclusions and Future Directions

References

[1]

[2] Animal pests: Poss.

[3] K Anderson, S. Hancock, M. Disney, and K.J. Gaston. Is waveform worth it? a comparison of lidar approaches for vegetation and landscape characterization. 2015.

[4] L Cao, N.C Coops, L.I. Innes, J. Dai, and H Ruan. Tree species classification in subtropical forests using small-footprint full-waveform lidar data. 2016.

[5] BBC Weather Centre. Climate change: Phenology.

[6] A. Chauve, C. Mallet, F. Bretar, S. Durrieu, M. Deseilligny, and W. Puech. Processing full-waveform lidar data: Modelling raw signals. *International Archives of Photogrammetry, Remote Sensing and Spatial Information Sciences*, 2007.

[7] Lindenmayer D. Gibbons P. *Tree Hollows and Wildlife Conservation in Australia.* CSIRO Publishing, 2002.

[8] R. L Goldingay. Characteristics of tree hollows used by australian birds and bats. *Wildlife Research*, 36(5):394–409, 2009.

[9] M Isenburg. *LAStools - efficient tools for LiDAR processing.* rapidlasso.

[10] B. Lawrie. *Beyond Angkor: How lasers revealed a lost city.* BBC News Magazine, 2014.

[11] D. B. Lindenmayer and J. T. Wood. Long-term patterns in the decay, collapse, and abundance of trees with hollows in the mountain ash (eucalyptus regnans) forests of victoria, southeastern australia. *Canadian Journal of Forest Research*, 40(1):48–54, 2010.

[12] C. Mallet and F. Bretar. Full-waveform topographic lidar: State-of-the-art. *ISPRS Journal of Photogrametry and Remote Sensing*, 64:1–16, 2009.

[13] M. Miltiadou, M. Warren, M. A.and Grant, and M. Brown. Alignment of hyperspectral imagery and full-waveform lidar data for visualisation and classification purposes. *The International Archives of Photogrammetry, Remote Sensing and Spatial Information Sciences*, 40(7):1257, 2015.

[14] A. Neuenschwander, L. Magruder, and M. Tyler. Landcover classification of small-footprint full-waveform lidar data. *Jounal of Applied Remote Sensing*, 3(1):033544–033544.

[15] A. Persson, U. Soderman, J. Topel, and S. Ahlberg. *Visualisation and Analysis of full-waveform airborne laser scanner data.* V/3 Workshop, Laser scanning 2005, 2005.

[16] J. Reitberger, P. Krzystek, and U. Stilla. Analysis of full waveform LiDAR data for tree species classification. *International Journal of Remote Sensing*, 29(5):1407–1431, 2008.

[17] R. B. Smith. *Introduction to Hyperspectral Imaging.* MicroImages, 2014.

[18] W. Wanger, A. Ullrich, V. Ducic, T. Maizer, and N. Studnicka. Gaussian decompositions and calibration of a novel small-footprint full-waveform digitising airborne laser scanner. *ISPRS Journal of Photogrammetry and Remote Sensing*, 60:100–112, 2006.

[19] W. Wanger, A. Ullrich, T. Melzer, C. Briese, and K. Kraus. From single-pulse to ful-waveform airborne laser scanners. *ISPRS Journal of Photogrammetry and Remote Sensing*, 60:100–112, 2004.

[20] A. Wehr and U. Lohr. Airborne laser scanning - an introduction and overview. *ISPRS Journal of Photogrammerty and Remote Sensing*, 54:68–82, 1999.

10 Appendices

10.1 Birds and Mammals Catalogue

10.1.1 Introduction

10.1.2 Australian arboreal Mammals

10.1.3 Australian Birds

The Forestry Corporation, Australia, provided a list of bird species that rely on hollows. But species are not limited to that list and more species rely uses hollows for shelters.

The provided list of the birds is divided into three groups:

1. Categorised as threatened species according to the Environement Protection and Biodiversity Conservation Act, 1999
Corella Eastern Rosella Superb Parrot Barking Owl Masked Owl

2. All the above species are included to the Action Plan for Australian Birds, 2000, as well as the following once:
Powerful Owl Sooty Owl

3. The rest:
Kookaburra Sulphur Crested Cockatoo Crimson Rosella Rainbow Lorikeet Musk Lorikeet Little Lorikeet Red-winged Parrot Cockatiel Australian Ringneck (Parrot) Red-rumped Parrot Powerful Owl Sooty Owl Barn Owl White-throated Treecreeper

10.1.4 Web-links of Photos

Mammals · Brush-tailed Possum - protected wildlife (Hollow: http://www.cavershamwildlife.com.au/comm
brushtail-possum/) (http://www.rymich.com/girraween/photos/animals/mammals/possums/trichos

Birds · Kookaburra (http://tenrandomfacts.com/blue-winged-kookaburra/) · Sulphur Crested Cockatoo (http://aussiegal7.deviantart.com/art/Sulphur-Crested-Cockatoo-08-15 · Corella (http://www.theparrotplace.co.nz/all-about-parrots/long-billed-corella/) · Crimson Rosella (http://25.media.tumblr.com/tumblr_m3mo89c40r1r4t9h1o1_1280.jpg) · Eastern Rosella (http://2.bp.blogspot.com/-pYxw51WjSOY/UB-LEFgd2KI/AAAAAAAAAWg/9z60PUWE6TE/s1600/_GJS6601-as-Smart-Object-1.jpg) · Galah (https://www.pinterest.com/pin/537546905498955709/) · Rainbow Lorikeet (https://www.reddit.com/r/pics/comments/328fvc/a_rainbow_lorikeet_found_in_coastal_regions/) · Musk Lorikeet ((http://www.rymich.com/girraween/photos/animals/birds/medium/glossopsitta_concinna/glossopsitta_concinna_001.jpg) · Little Lorikeet (http://www.pbase.com/sjmurray/psittacidae) · Red-winged Parrot (https://www.pinterest.com/pin/395894623469889727 · Superb Parrot (http://www.davidkphotography.com/?showimage=637) · Cockatiel (http://up.parsipet.ir/uploads/Cockatiels-for-sale.jpg) · Australian Ringneck (Parrot) (http://ontheroadmagazine.com.au/wp-content/uploads/2015/09/Twenty-eight-parrot- jpg) · Red-rumped Parrot (http://parrotfacts.net/wp-content/uploads/Red-Rumped-Parrot-on-a jpg) · Powerful Owl (http://farm1.staticflickr.com/219/495796536_f78dac04c1.jpg) · Sooty Owl (hollow: http://www.mariewinn.com/marieblog/uploaded_images/screech2-738532.jpg) (http://www.owlpages.com/owls/species/images/greater_sooty_owl_richard_jackson-1.jpg) · Barking Owl (http://www.pcpimages.com/Nature-and-Wildli Birds/i-7JKSTp5/1/L/owl%20%281%20of%201%29-L.jpg) · Masked Owl (http://www.survival.org.au/images/birds/masked_owl_2_600.jpg) · Barn Owl (Hollow: http://www.barnowltrust.org.uk/wp-content/uploads/Barn_Owl_hollow_tree-wallpaper.jpg) (https://upload.wikimedia.org/wikipedia/commons/c/c6/Tyto_alba_-British_Wildlife_Centre,_Surrey,_England-8a_%281%29.jpg)

· White-throated Treecreeper (http://www.birdlifemelbourne.org.au/bird-lists/47-Treecreepers/White-throated-Treecreeper/White-throated%20Treecreeper%202%20JB.jpg) (hollow: https://geoffpark.files.wordpress.com/2011/09/female-white-throated-treecreeper.jpg)

Hollow Owl : http://www.mariewinn.com/marieblog/uploaded_images/screech2-738532.jpg